Pre-COSTAR FOS Aperture Transmissions for Point Sources and Surface Brightness of Diffuse Sources[1]

R. C. Bohlin[2]

Abstract

The FOS absolute sensitivities are determined by observations of standard stars in the 4.3 arcsec acquisition aperture. For estimates of absolute fluxes of point sources that are observed in smaller apertures, the apparent, measured transmission of the smaller aperture relative to the 4.3 arcsec aperture is required. Proposal 4211 was designed to extend our knowledge of these aperture corrections and to verify the stability of the throughput relative to earlier measurements by proposal 3106 in 1991. Despite a lack of a theoretical explanation, the data demonstrate that the aperture corrections depend on the detector and grating and, therefore, differ from the true transmission of the aperture, which is a function of only the aperture size and the PSF at the relevant wavelength.

The formula for computing the specific intensity of sources of diffuse surface brightness depends on the absolute fractional transmission of the 4.3 aperture for a point source but NOT on the aperture correction for a smaller observation aperture.

I. Observations

In order to compute the relative aperture throughput, the count rate spectrum in the smaller apertures is divided by the countrate spectrum of the same star in the A1(4.3 arcsec) aperture. All of the mean measured aperture corrections in Table 1 are derived from countrates that are corrected to the optimal (zero) OTA focus position according to step 1 of the prescription of Lindler & Bohlin (1993), which is an improvement on the focus correction used to compute the corresponding throughput ratios that appeared in Table 4 of Neil, Bohlin & Hartig (1992); hereafter NBH. The OTA focus was +10 microns on 1991.43 for the Prop 3106 blue side data, −4 microns on 1991.96 for the Prop 3106 red side data, and −3.5 microns for the Prop 4211 measurements on 1992.77. The maximum focus corrections are on 1991.43 for the blue side, where the B2(0.3 arcsec) correction is .92 for the short wavelength gratings H13 and L15 but is less than 5 percent for the other gratings. For the larger apertures, the correction from +10 to 0 microns is less than 3 percent, so that errors in the correction procedure cannot cause anomalies larger than 1-2 percent. The data are recorded at three ybase positions perpendicular to the dispersion and verify the photometric precision, despite the ybase positioning errors discovered by Koratkar

1. Originally published as FOS Instrument Science Report CAL/FOS-106.
2. Space Telescope Science Institute, Baltimore, MD 21218

and Taylor (1993). The values in Table 1 represent the average ratio of the mean spectrum in the designated aperture divided by the mean spectrum in the A1 (4.3 arcsec) aperture, as discussed in more detail by NBH.

Table 1: Mean Aperture Throughput Ratios

Grat	B3 (1 arcsec) Blue	B3 (1 arcsec) Red	B1 (0.5 arcsec) Blue	B1 (0.5 arcsec) Red	B2 (0.3 arcsec) Blue	B2 (0.3 arcsec) Red	C2-SLIT Blue	C2-SLIT Red
H13	0.59	—	0.40	—	0.26	—	0.39	—
H13 [a]	0.58	—	—	—	—	—	—	—
H19	0.60	0.60	0.42	0.44	0.26	0.31 [b]	0.39	0.41
H19 [c]	0.57	0.60	0.41	0.40 [d]	0.29	0.21 [d]	0.40	0.42
H19 [a]	0.58							
H27	0.57	0.59	0.42	0.44	0.26	0.32	0.39	0.42
H27 [a]	0.57							
H40	0.57	0.61	0.42	0.44	0.27	0.32	0.38	0.42
H57	—	0.59	—	0.44	—	0.31	—	0.41
H78	—	0.58	—	0.43	—	0.28	—	0.39
L15	0.65	0.67	0.46	0.50	0.31	0.30 [b]	0.42	0.45
L15 [c]	0.64 [b]	0.66	0.46	0.44 [d]	0.32	0.25 [d]	0.44	0.45
L65	—	0.67	—	0.51	—	0.35	—	0.45
PRI [c]	0.53	0.54	0.37	0.36 [d]	0.26	0.20 [d]	0.37	0.39

a. prop 3235
b. Ystep repeatability worse than 3 percent. Excess jitter or ybase error.
c. prop 4211. Otherwise prop 3106.
d. Bad target acquisition. Use as lower limits.

The target acquisition for these data consists of a four stage peakup, where the final stage is in the B2(0.3 arcsec) aperture on 0.05 arcsec centers in order to limit the pointing uncertainty to 0.025 arcsec in each axis. There is an additional pointing tweak in the slit on 0.05 arcsec centers in the X axis only. During the side switch from blue to red in prop 4211, only the final stage of the peakup was done in the B2(0.3 arcsec) aperture. Unfortunately, the extent of this raster pattern was insufficient to account for the uncertainty in the offset between the sides and resulted in a pointing error of about 0.12 arcsec (Bohlin 1993). This 0.12 arcsec error means that the red side measurements in 4211 for the 0.5 arcsec and the 0.3 arcsec apertures are spuriously low. The subsequent red slit tweak up corrected the pointing error for the red side slit observations.

II. Comparison with models

Table 2 summarizes the expected aperture transmission of the four commonly used apertures relative to the A1(4.3 arcsec) aperture at optimal OTA focus, as derived from the Table 2 of Lindler & Bohlin (1993), who used the TIM software of Burrows & Hasan (1993) to estimate the aberrated PSF at the FOS entrance apertures. The weak wavelength dependence is caused by the change in the modeled PSF with wavelength and is <2 percent for the B3(1 arcsec) and slit over the most relevant wavelength range of 1400 to 5000Å on the blue side. The B2(0.3 arcsec) increases by 4 percent, while a drop of 10 percent is predicted for B1(0.5 arcsec) over the same range. Differences of a few percent between Table 2 and the relative transmissions of Evans (1993) are indicative of the fidelity of the TIM model PSFs. In order to compare the data with the theory, Table 3 contains the ratios of the measurements of Table 1 to the predictions of Table 2. The lower limits are omitted in Table 3.

Table 2: Relative Aperture Transmission From TIM Theory at OTA Nominal Focus

Grat	WL	Blue	Red	Blue	Red	Blue	Red	Blue	Red
		B3 (1arcsec)		B1 (0.5 arcsec)		B2 (0.3 arcsec)		C2-SLIT	
H13	1400	.618	—	.483	—	.314	—	.427	—
H19	2000	.614	.612	.473	.475	.315	.317	.425	.414
H27	3000	.610	.610	.462	.462	.316	.320	.423	.415
H40	4000	.610	.609	.450	.450	.322	.323	.422	.415
H57	5000	.609	.607	.438	.437	.327	.326	.422	.416
H78	8000	—	.614	—	.437	—	.303	—	.407
L15	2000	.614	.612	.473	.475	.315	.317	.425	.414
L65	5000	.609	.607	.438	.437	.327	.326	.422	.416
PRI	3000	.610	.610	.462	.462	.316	.320	.423	.415

III. Discussion and Recommendations

The aperture corrections are difficult to measure to a 1 percent accuracy because of GIMP (Fitch et al. 1993; and see this volume), pointing errors, OTA breathing, jitter, and ybase errors. Even though many of the deviations from unity in Table 3 cannot be explained by these difficulties, the statistical significance of the deviations of the data from the predictions seems undeniable. In particular, consider the differences between the red and blue sides for the high dispersion H gratings. For the 14 cases where the same grating is measured on both sides, all of the red side values exceed the blue measurements, except for one case of equal throughput. This difference is not predicted by the theory; and the predicted 10 percent drop with wavelength for B1 is not observed, i.e. the measurements of Table 1 are nearer to being constant than the ratios to the theory in Table 3. The TIM output images have a strong resemblance to actual PSFs but are known to suffer some serious imperfections, especially for some non-prime *HST* camera modes such as PC8. The uncertainties in the model PSFs at the FOS entrance apertures are not quantified and cannot be the basis for the recommended final aperture corrections.

The following is a case-by-case discussion for each aperture-grating combination. These recommended aperture corrections are summarized in Table 4.

Table 3: Measured Throughput Relative to Theoretical Value

Grat	Blue	Red	Blue	Red	Blue	Red	Blue	Red
	B3 (1 arcsec)		B1 (0.5 arcsec)		B2 (0.3 arcsec)		C2-SLIT	
H13	0.95	—	0.83	—	0.83	—	0.91	—
H19	0.98	0.98	0.89	0.93	0.83	0.98	0.92	0.99
H19 [a]	0.93	0.98	0.87	—	0.92	—	0.94	1.01
H27	0.93	0.97	0.91	0.95	0.82	1.00	0.92	1.01
H40	0.93	1.00	0.93	0.98	0.84	0.99	0.90	1.01
H57	—	0.97	—	1.01	—	0.95	—	0.99
H78	—	0.94	—	0.98	—	0.92	—	0.96
L15	1.06	1.09	0.97	1.05	0.98	0.95	0.99	1.09
L15 [a]	1.04	1.08	0.97	—	1.02	—	1.04	1.09
L65	—	1.10	—	1.17	—	1.07	—	1.08
PRI [a]	0.87	0.89	0.80	—	0.82	—	0.87	0.94

a. prop=4211. Otherwise prop=3106

Table 4: Recommended Aperture Corrections and Uncertainties at Nominal OTA Focus

GRAT MODE	Blue	Red	Unc [a]	Blue	Red	Unc	Blue	Red	Unc	Blue	Red	Unc
	B3 (1 arcsec)			B1 (0.5 arcsec)			B2 (0.3 arcsec)			C2-SLIT		
HIGH	0.58	0.60	.02	0.41	0.44	.02	0.27	0.31	.03	0.39	0.41	.02
LOW	0.65	0.67	.06	0.46	0.50	.04	0.31	0.35	.03	0.43	0.45	.03
PRISM	0.53	0.54	.06	0.37	0.39	.04	0.26	0.30	.03	0.37	0.39	.03

a. The uncertainties (Unc) do not include the possible contributions of pointing errors, OTA "breathing," jitter, or ybase errors in an arbitrary science observation.

High Dispersion

The small scatter in each of the 8 columns of data for the H gratings in Table 1 suggests that an average of each column might reduce the uncertainties further. An exception is H78, which is slightly low in all four cases

B3 (1 arcsec)

The blue side average is 0.58 with a maximum deviation of 0.02 or 3 percent, while the red side mean is 0.60 with 0.02 uncertainty. The excluded measurement for H78 is within the 3 percent uncertainty.

B1 (0.5 arcsec)

The blue side average is 0.41 with a maximum deviation of 0.01 or 2 percent, while the red side mean is 0.44 with no scatter among the 4 valid entries. A reasonable error estimate might be 3 percent. The excluded measurement for H78 is within the uncertainty.

B2 (0.3 arcsec)

The blue side average is 0.27 with a maximum deviation of 0.02 or 7 percent, while the red side mean is 0.31 with 0.01 scatter among the 4 valid entries. The excluded measurement for H78 is 10 percent lower than the average; and 10 percent might be a good choice for an uncertainty, since this small aperture is most susceptible to pointing problems and jitter. For precise absolute flux measurements of point sources, a larger aperture should be used.

C2 (0.25x2 slit)

The blue side average is 0.39 with a maximum deviation of 0.01 or 3 percent, while adopting a red side mean of 0.41 with a nominal 5 percent or 0.02 uncertainty encompasses the H78 measurement.

Low Dispersion

Because of the extreme differences that approach 20 percent between the prism and the L15 measurements, one case of the blue B3(1 arcsec) aperture is investigated in detail. Pointing errors and jitter problems are minimal for this aperture. Only the L15 spectrum in B3 for prop 4211 shows a spread in the three different Y-base countrates as large as 3 percent. Y-base errors can only cause a loss of signal, so the aperture correction of 0.64 could be a lower limit but is too large already in comparison with the prism value of 0.53 for the same aperture. The other known effect on aperture transmission is OTA "breathing", i.e. short term OTA focus changes, which are observed to deviate from the nominal by 5 microns during an orbit. However, the A1 reference spectra for the prism and L15 were taken only 4 min apart, while the B3 spectra were also separated by a 4 min time interval. A shift in OTA focus of at least 30 microns in 4 min would be required to cause the observed difference in transmission! Therefore, differences in aperture corrections among dispersing elements must be accepted along with the differences between the blue and red sides.

B3 (1 arcsec)

For L15 on the blue side, 0.65 is recommended because of the possible Y-base error for the other measurement of 0.64, while the red side mean for L15 and L65 is 0.67 with 0.01 scatter. There are only single measurements for the prism. These values differ by around 10 percent from the high dispersion values, so 10 percent seems like a safe uncertainty estimate.

B1 (0.5 arcsec)

For L15 on the blue side, 0.46 is the value for both entries in Table 1, while 0.50 is suggested for the red side L15 and L65. There is no valid measurement for the red side prism, so the blue side is scaled up by the typical difference from the blue to the red side. Again, 10 percent seems like a safe uncertainty estimate.

B2 (0.3 arcsec)

For L15 on the blue side, 0.31 is the smaller of the two entries in Table 1, while 0.35 is the one valid entry for L65. There is no valid measurement for the red side prism, so the blue side is scaled up by the 0.04 difference between red and blue for the gratings. Again, 10 percent seems like a safe uncertainty estimate.

C2 (0.25x2 arcsec slit)

The blue side L15 average is 0.43 with a deviation of 0.01 or 3 percent, while all three L values on the red side are 0.45. Symmetry with respect to high and low dispersion for the B1(0.5 arcsec) aperture suggests that the prism corrections for the slit might be 0.02 lower than the quoted values from the single measurements, so 0.03 should be a safe error estimate.

IV. Wavelength Dependence Within the Range of a Single Disperser

According to the theoretical predictions, the variation in the aperture correction within the wavelength range covered by a grating is always less than the ~4 percent for the B1 (0.5 arcsec) aperture on the blue L15. For the broad coverage of the prisms, the predicted variation with wavelength approaches 10 percent. NBH (1992) fit straight lines or quadratics to the aperture corrections as a function of wavelength. Table 5 summarizes the slope of the curve in terms of the ratio of the longest wavelength fit point to the first fit point for the quadratic fits. The aperture corrections do not agree with the predicted transmissions, for example the measured slope for the case of B1(0.5 arcsec)-blue-L15 is 1.03-1.06 in Table 5, while the TIM prediction is ~0.96. Therefore, the question of wavelength dependence must be answered by the data. One of the main purposes of prop 4211 was to check the repeatability of these slopes that were first measured in prop 3106 by NBH. The slopes did repeat for the test cases of H19 and L15 to an accuracy of 6 percent. Unfortunately, a couple of the more important cases in the B3 aperture for H13 (0.91) and H27 (0.92) on the blue side show more than a 6 percent deviation from unity and confirm the necessity of aperture correction that vary with wavelength.

Table 5: Slopes of Aperture Ratios Across Each Spectrum

Grat	B3 (1 arcsec)		B1 (0.5 arcsec)		B2 (0.3 arcsec)		C2-SLIT	
	Blue	Red	Blue	Red	Blue	Red	Blue	Red
H13	0.91	0.00	0.89	0.00	1.00	0.00	0.96	0.00
H13 [a]	0.90							
H19	0.98	0.99	1.05	1.06	1.05	1.06	1.06	1.04
H19 [b]	0.96	1.02	1.00	1.04	1.04	1.13 [c]	1.01	1.01
H19 [a]	0.97							
H27	0.92	0.95	0.97	0.97	0.97	0.95	0.98	0.97
H27 [a]	0.93							
H40	0.94	0.97	0.94	0.94	0.96	0.97	0.96	0.97
H57	0.00	1.01	0.00	1.02	0.00	0.93	0.00	0.95
H78	0.00	0.96	0.00	1.01	0.00	0.88	0.00	0.94
L15	0.96	0.89	1.06	0.95	1.17	0.94	1.07	0.97
L15 [b]	0.96	0.94	1.03	0.98	1.11	0.95 [c]	1.08	0.91
L65	0.00	0.98	0.00	1.00	0.00	0.95	0.00	0.95
PRI [b]	0.98	1.19	1.02	1.05	1.06	1.04	1.04	1.12

a. prop 3235.
b. prop 4211. Otherwise prop 3106.
c. Bad target acquisition. Do not use for final average polynomial fits.

A search of the archive revealed one more prop 3235, which again verifies the repeatability of both the aperture correction and the slope for the important cases of B3(1 arcsec) on the blue side for H13, H19, and H27. In comparison with the adopted value of 0.58 in Table 4, the 3235 data for the aperture corrections are 0.58, 0.58, and 0.57, respectively. All three slopes are within 1 percent of the values in Table 5! Therefore, the existence of the slopes found by NBH is verified. The aperture corrections are derived from the least square fit of quadratic polynomials as a function of wavelength. For some FOS dispersers that have a rapid drop in sensitivity, separate secondary quadratic fits are required and improve on the single

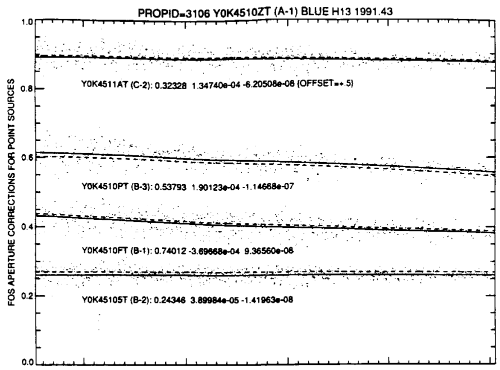
PROPID=3106 Y0K4510ZT (A-1) BLUE H13 1991.43
FOS APERTURE CORRECTIONS FOR POINT SOURCES
Y0K4511AT (C-2): 0.32328 1.34740e-04 -6.20508e-08 (OFFSET=+.5)
Y0K4510PT (B-3): 0.53793 1.90123e-04 -1.14668e-07
Y0K4510FT (B-1): 0.74012 -3.69668e-04 9.36560e-08
Y0K45105T (B-2): 0.24346 3.89984e-05 -1.41963e-08

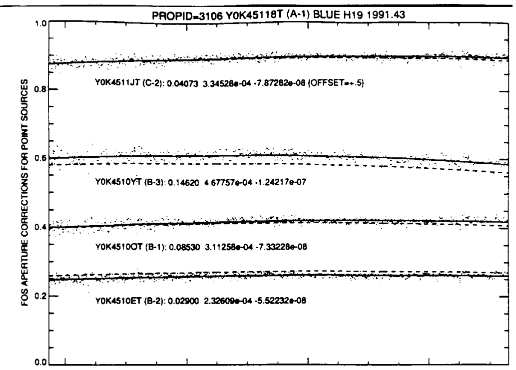
PROPID=3106 Y0K45118T (A-1) BLUE H19 1991.43
FOS APERTURE CORRECTIONS FOR POINT SOURCES
Y0K4511JT (C-2): 0.04073 3.34528e-04 -7.87282e-08 (OFFSET=+.5)
Y0K4510YT (B-3): 0.14620 4.67757e-04 -1.24217e-07
Y0K4510OT (B-1): 0.08530 3.11258e-04 -7.33228e-08
Y0K4510ET (B-2): 0.02900 2.32609e-04 -5.52232e-08

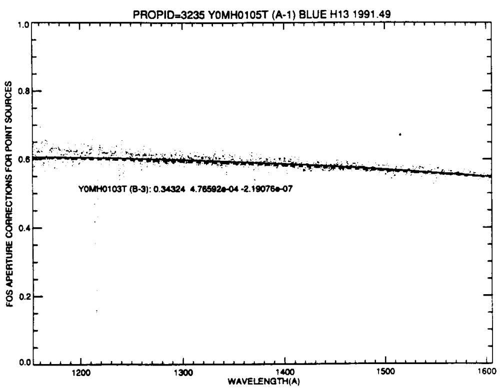
PROPID=3235 Y0MH0105T (A-1) BLUE H13 1991.49
FOS APERTURE CORRECTIONS FOR POINT SOURCES
Y0MH0103T (B-3): 0.34324 4.76592e-04 -2.19076e-07
WAVELENGTH(A)

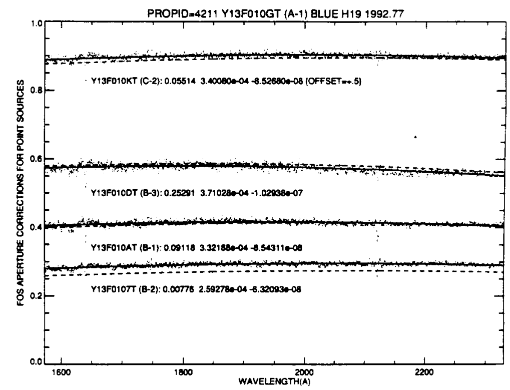
PROPID=4211 Y13F010GT (A-1) BLUE H19 1992.77
FOS APERTURE CORRECTIONS FOR POINT SOURCES
Y13F010KT (C-2): 0.05514 3.40080e-04 -8.52680e-08 (OFFSET=+.5)
Y13F010DT (B-3): 0.25291 3.71028e-04 -1.02938e-07
Y13F010AT (B-1): 0.09118 3.32188e-04 -8.54311e-08
Y13F0107T (B-2): 0.00776 2.59278e-04 -6.32093e-08
WAVELENGTH(A)

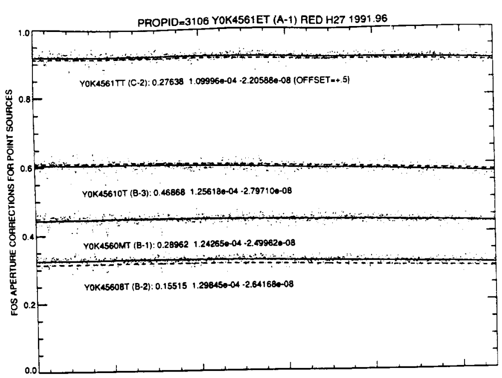
PROPID=3106 Y0K4561ET (A-1) RED H27 1991.96
FOS APERTURE CORRECTIONS FOR POINT SOURCES
Y0K4561TT (C-2): 0.27638 1.09996e-04 -2.20588e-08 (OFFSET=+.5)
Y0K45610T (B-3): 0.46868 1.25618e-04 -2.79710e-08
Y0K4560MT (B-1): 0.28962 1.24265e-04 -2.49962e-08
Y0K45608T (B-2): 0.15515 1.29845e-04 -2.64168e-08

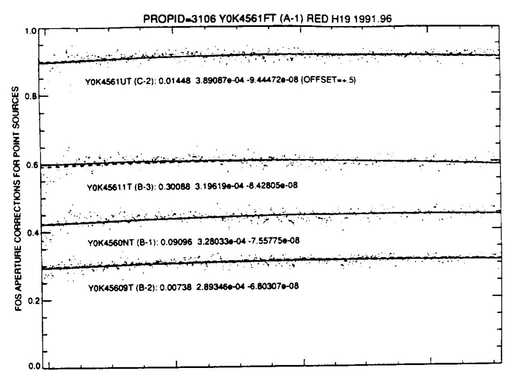
PROPID=3106 Y0K4561FT (A-1) RED H19 1991.96
FOS APERTURE CORRECTIONS FOR POINT SOURCES
Y0K4561UT (C-2): 0.01448 3.89087e-04 -9.44472e-08 (OFFSET=+.5)
Y0K45611T (B-3): 0.30088 3.19619e-04 -8.42805e-08
Y0K4560NT (B-1): 0.09096 3.28033e-04 -7.55775e-08
Y0K45609T (B-2): 0.00738 2.89346e-04 -6.80307e-08

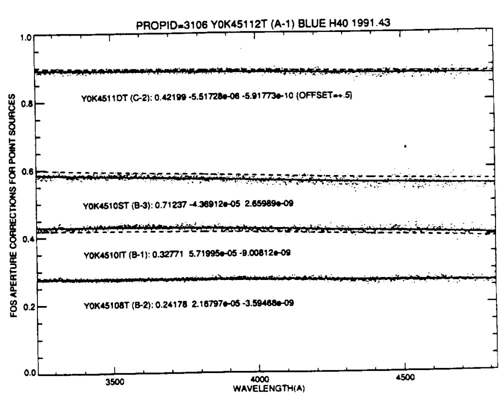
PROPID=3106 Y0K45112T (A-1) BLUE H40 1991.43
FOS APERTURE CORRECTIONS FOR POINT SOURCES
Y0K4511DT (C-2): 0.42199 -5.51728e-06 -5.91773e-10 (OFFSET=+.5)
Y0K4510ST (B-3): 0.71237 -4.36912e-05 2.65989e-09
Y0K4510IT (B-1): 0.32771 5.71995e-05 -9.00812e-09
Y0K45108T (B-2): 0.24178 2.16797e-05 -3.59468e-09
WAVELENGTH(A)

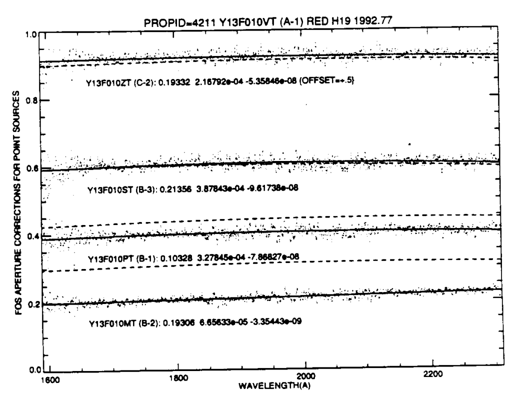
PROPID=4211 Y13F010VT (A-1) RED H19 1992.77
FOS APERTURE CORRECTIONS FOR POINT SOURCES
Y13F010ZT (C-2): 0.19332 2.16792e-04 -5.35846e-08 (OFFSET=+.5)
Y13F010ST (B-3): 0.21356 3.87843e-04 -9.61738e-08
Y13F010PT (B-1): 0.10328 3.27845e-04 -7.88827e-08
Y13F010MT (B-2): 0.19306 6.65633e-05 -3.35443e-09
WAVELENGTH(A)

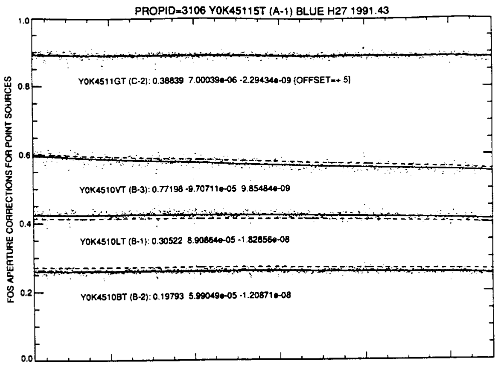
PROPID=3106 Y0K45115T (A-1) BLUE H27 1991.43
FOS APERTURE CORRECTIONS FOR POINT SOURCES
Y0K4511GT (C-2): 0.38839 7.00039e-06 -2.29434e-09 (OFFSET=+.5)
Y0K4510VT (B-3): 0.77198 -9.70711e-05 9.85484e-09
Y0K4510LT (B-1): 0.30522 8.90864e-05 -1.82856e-08
Y0K4510BT (B-2): 0.19793 5.99049e-05 -1.20871e-08

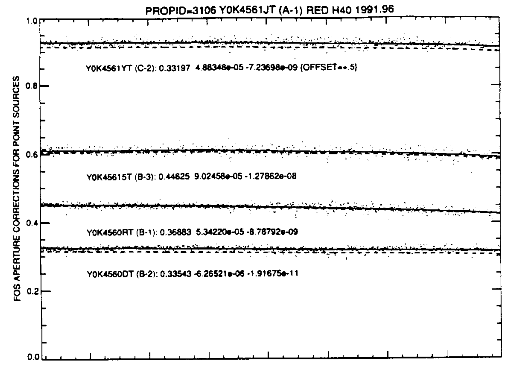
PROPID=3106 Y0K4561JT (A-1) RED H40 1991.96
FOS APERTURE CORRECTIONS FOR POINT SOURCES
Y0K4561YT (C-2): 0.33197 4.88348e-05 -7.23698e-09 (OFFSET=+.5)
Y0K45615T (B-3): 0.44625 9.02458e-05 -1.27862e-08
Y0K4560RT (B-1): 0.36883 5.34220e-05 -8.78792e-09
Y0K4560DT (B-2): 0.33543 -6.26521e-06 -1.91675e-11

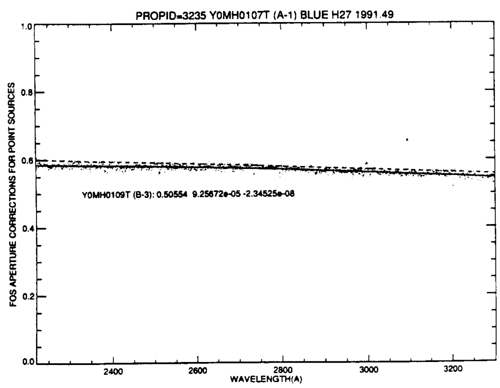
PROPID=3235 Y0MH0107T (A-1) BLUE H27 1991.49
FOS APERTURE CORRECTIONS FOR POINT SOURCES
Y0MH0109T (B-3): 0.50554 9.25672e-05 -2.34525e-08
WAVELENGTH(A)

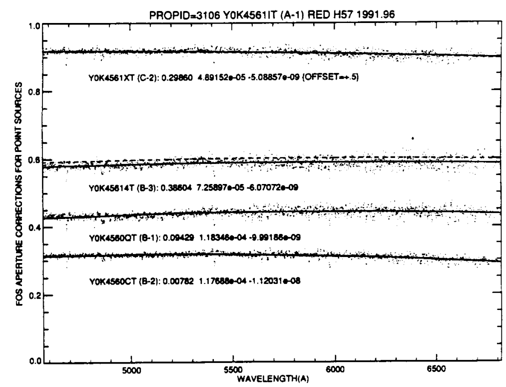
PROPID=3106 Y0K4561IT (A-1) RED H57 1991.96
FOS APERTURE CORRECTIONS FOR POINT SOURCES
Y0K4561XT (C-2): 0.29860 4.89152e-05 -5.08857e-09 (OFFSET=+.5)
Y0K45614T (B-3): 0.38604 7.25897e-05 -6.07072e-09
Y0K4560QT (B-1): 0.09429 1.18346e-04 -9.99186e-09
Y0K4560CT (B-2): 0.00782 1.17688e-04 -1.12031e-08
WAVELENGTH(A)

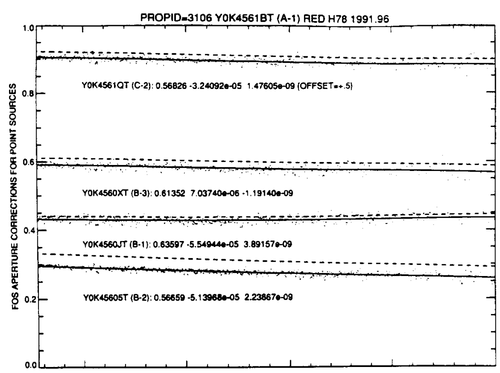
PROPID=3106 Y0K4561BT (A-1) RED H78 1991.96
FOS APERTURE CORRECTIONS FOR POINT SOURCES
Y0K4561QT (C-2): 0.56826 -3.24092e-05 1.47605e-09 (OFFSET=+.5)
Y0K4560XT (B-3): 0.61352 7.03740e-06 -1.19140e-09
Y0K4560JT (B-1): 0.63597 -5.54944e-05 3.89157e-09
Y0K45605T (B-2): 0.56659 -5.13968e-05 2.23867e-09

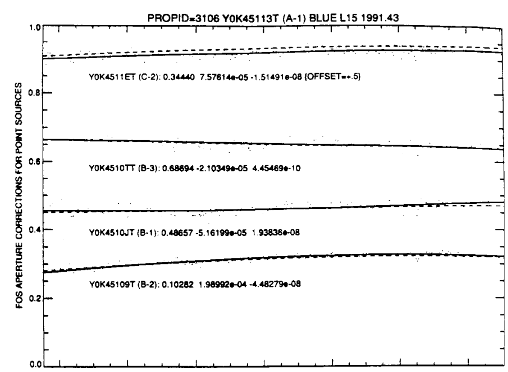
PROPID=3106 Y0K45113T (A-1) BLUE L15 1991.43
FOS APERTURE CORRECTIONS FOR POINT SOURCES
Y0K4511ET (C-2): 0.34440 7.57614e-05 -1.51491e-08 (OFFSET=+.5)
Y0K4510TT (B-3): 0.68694 -2.10349e-05 4.45469e-10
Y0K4510JT (B-1): 0.48657 -5.16199e-05 1.93836e-08
Y0K45109T (B-2): 0.10282 1.98992e-04 -4.48279e-08

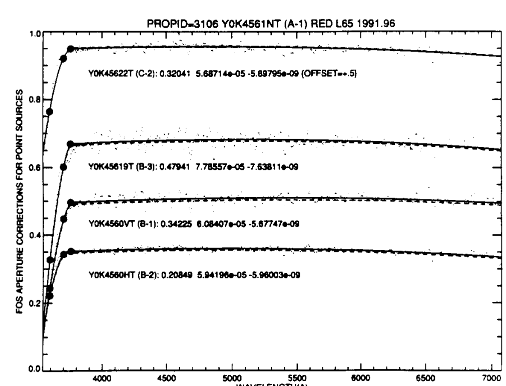
PROPID=3106 Y0K4561NT (A-1) RED L65 1991.96
FOS APERTURE CORRECTIONS FOR POINT SOURCES
Y0K45622T (C-2): 0.32041 5.68714e-05 -5.89795e-09 (OFFSET=+.5)
Y0K45619T (B-3): 0.47941 7.78557e-05 -7.63811e-09
Y0K4560VT (B-1): 0.34225 6.08407e-05 -5.67747e-09
Y0K4560HT (B-2): 0.20849 5.94196e-05 -5.96003e-09
WAVELENGTH(A)

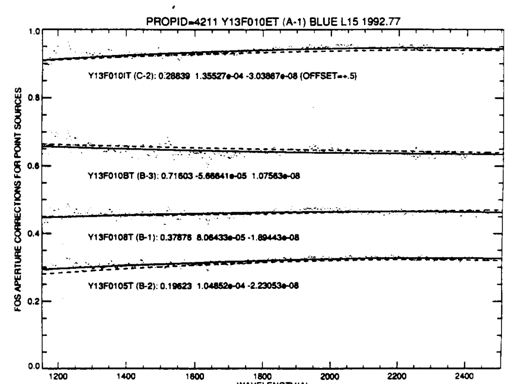
PROPID=4211 Y13F010ET (A-1) BLUE L15 1992.77
FOS APERTURE CORRECTIONS FOR POINT SOURCES
Y13F010IT (C-2): 0.28839 1.35527e-04 -3.03867e-08 (OFFSET=+.5)
Y13F010BT (B-3): 0.71603 -5.66641e-05 1.07563e-08
Y13F0108T (B-1): 0.37876 8.06433e-05 -1.89443e-08
Y13F0105T (B-2): 0.19623 1.04852e-04 -2.23053e-08
WAVELENGTH(A)

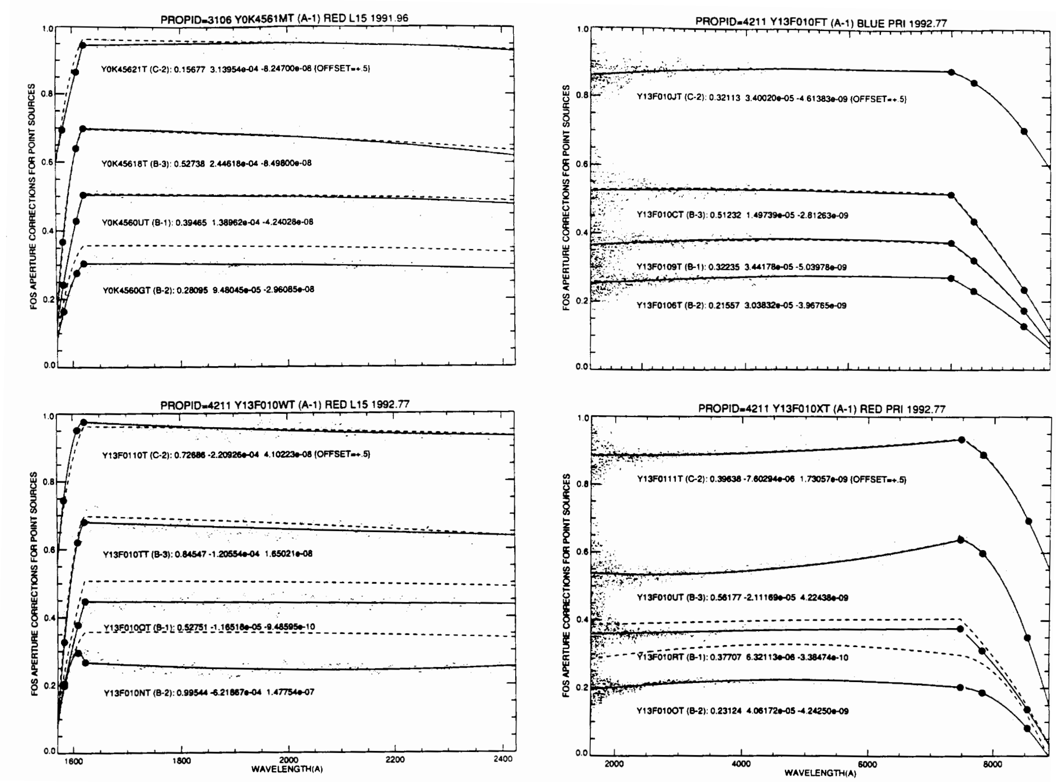

Figure 1

fit reported by NBH. These cases that show a discontinuity in the aperture corrections are caused by the broad aberrated PSF in the 4.3 arcsec aperture that results in a slower drop with wavelength in the A1(4.3 arcsec) aperture than for the smaller apertures. The fits are all shown as the solid line in Figure 1; and the second fit is defined by the three large filled circles. One of the three filled circles always lies at the endpoint of first fit in order to force continuity between the two quadratics. The other two filled circles are the binned averages of the remaining data points. The dashed lines are the adopted average fit, as described in the next paragraph.

The final adopted aperture corrections are the averages of the coefficients from the quadratic fits for the individual measurement sets, where the individual fits are first normalized to the average corrections of Table 4 over the wavelength range of the primary fit. The individual coefficients of the primary fits are written on the plots in Figure 1, while Table 6 contains the applicable wavelength range and number of data sets used to define each set of three average coefficients. The two of the three most discrepant observations in the small B2(0.3 arcsec) aperture from prop 4211 are excluded from the averaging process for the bad target acquisition on the red side. The H19 and L15 are excluded, while the prism must be used, since 4211 contained the only data available for the prism aperture corrections.

Table 6: Summary of average FOS Aperture Coefficients [a]

Detec	FGWA	APER	C0	C1	C2	WMIN	WMAX	NAV
BLUE	H13	B-1	7.40123e-01	−3.69668e −04	9.36560e −08	1151.00	1609.00	1
BLUE	H13	B-2	2.43460e −01	3.89984e −05	−1.41963e −08	1151.00	1609.00	1
BLUE	H13	B-3	4.40583e −01	3.33357e −04	−1.66872e −07	1151.00	1610.00	2
BLUE	H13	C-2	3.23279e −01	1.34740e −04	−6.20508e −08	1151.00	1610.00	1
BLUE	H19	B-1	8.82408e −02	3.21723e −04	−7.93770e −08	1567.00	2335.00	2
BLUE	H19	B-2	1.83798e −02	2.45943e −04	−5.92163e −08	1567.00	2335.00	2
BLUE	H19	B-3	2.30025e −01	3.88200e −04	−1.05693e −07	1567.00	2335.00	3
BLUE	H19	C-2	4.79387e −02	3.37304e −04	−8.19981e −08	1567.00	2335.00	2
BLUE	H27	B-1	3.05223e −01	8.90864e −05	−1.82856e −08	2213.00	3308.00	1
BLUE	H27	B-2	1.97932e −01	5.99049e −05	−1.20871e −08	2214.00	3308.00	1
BLUE	H27	B-3	6.38760e −01	−2.25195e −06	−6.79883e −09	2213.00	3308.00	2
BLUE	H27	C-2	3.88393e −01	7.00039e −06	−2.29434e −09	2213.00	3308.00	1
BLUE	H40	B-1	3.27705e −01	5.71995e −05	−9.00812e −09	3229.00	4830.00	1
BLUE	H40	B-2	2.41780e −01	2.16797e −05	−3.59468e −09	3229.00	4830.00	1
BLUE	H40	B-3	7.12372e −01	−4.36912e −05	2.65989e −09	3229.00	4830.00	1
BLUE	H40	C-2	4.21993e −01	−5.51728e −06	−5.91773e −10	3229.00	4830.00	1
BLUE	L15	B-1	4.32666e −01	1.451 17e −05	2.19650e −10	1151.00	2523.00	2
BLUE	L15	B-2	1.49524e −01	1.51922e −04	−3.35666e −08	1151.00	2523.00	2
BLUE	L15	B-3	7.01490e −01	−3.88495e −05	5.60088e −09	1151.00	2523.00	2
BLUE	L15	C-2	3.16397e −01	1.05644e −04	−2.27679e −08	1151.00	2523.00	2
BLUE	PRI	B-1	3.22353e −01	3.44178e −05	−5.03978e −09	1498.00	4995.00	1
BLUE	PRI	B-1	−1.21560e+00	8.38476e −04	−1.04393e −07	4993.00	5961.00	1
BLUE	PRI	B-2	2.15567e −01	3.03832e −05	−3.96765e −09	1498.00	4995.00	1
BLUE	PRI	B-2	−4.04202e −01	4.26773e −04	−5.85007e −08	4993.00	5961.00	1
BLUE	PRI	B-3	5.12325e −01	1.49739e −05	−2.81263e −09	1498.00	4995.00	1
BLUE	PRI	B-3	−3.05272e −02	5.52881e −04	−8.87815e −08	4993.00	5961.00	1
BLUE	PRI	C-2	3.21 130e −01	3.40020e −05	−4.61383e −09	1498.00	4995.00	1
BLUE	PRI	C-2	−4.03502e+00	1.87340e −03	−1.98278e −07	4993.00	5961.00	1
AMBER	H19	B-1	9.71 168e −02	3.27939e −04	−7.71301e −08	1588.00	2316.00	2
AMBER	H19	B-2	7.38173e −03	2.89346e −04	−6.80307e −08	1588.00	2317.00	1

Table 6: Summary of average FOS Aperture Coefficients [a]

Detec	FGWA	APER	C0	C1	C2	WMIN	WMAX	NAV
AMBER	H19	B-3	2.57219e −01	3.53731e −04	−9.02272e −08	1588.00	2316.00	2
AMBER	H19	C-2	1.03904e −01	3.02940e −04	−7.40159e −08	1588.00	2316.00	2
AMBER	H27	B-1	2.89623e −01	1.24265e −04	−2.49962e −08	2217.00	3284.00	1
AMBER	H27	B-2	1.55147e −01	1.29845e −04	−2.64168e −08	2217.00	3283.00	1
AMBER	H27	B-3	4.68684e −01	1.25618e −04	−2.79710e −08	2217.00	3284.00	1
AMBER	H27	C-2	2.76376e −01	1.09996e −04	−2.20588e −08	2217.00	3284.00	1
AMBER	H40	B-1	3.68828e −01	5.34220e −05	−8.78792e −09	3226.00	4791.00	1
AMBER	H40	B-2	3.35431e −01	−6.26521e −06	−1.91675e −11	3226.00	4791.00	1
AMBER	H40	B-3	4.46254e −01	9.02458e −05	−1.27862e −08	3229.00	4790.00	1
AMBER	H40	C-2	3.31970e −01	4.88348e −05	−7.23698e −09	3226.00	4788.00	1
AMBER	H57	B-1	9.42854e −02	1.18346e −04	−9.99186e −09	4559.00	6829.00	1
AMBER	H57	B-2	7.82160e −03	1.17688e −04	−1.12031e −08	4559.00	6829.00	1
AMBER	H57	B-3	3.86043e −01	7.25897e −05	−6.07072e −09	4561.00	6831.00	1
AMBER	H57	C-2	2.98603e −01	4.89152e −05	−5.08857e −09	4561.00	6829.00	1
AMBER	H78	B-1	6.35974e −01	−5.54944e −05	3.89157e −09	6260.00	8501.00	1
AMBER	H78	B-2	5.66594e −01	−5.13968e −05	2.23867e −09	6263.00	8501.00	1
AMBER	H78	B-3	6.13518e −01	7.03740e −06	−1.19140e −09	6260.00	8501.00	1
AMBER	H78	C-2	5.68258e −01	−3.24092e −05	1.47605e −09	6263.00	8501.00	1
AMBER	L15	B-1	4.61080e −01	6.36551e −05	−2.16757e −08	1619.00	2444.00	2
AMBER	L15	B-1	−1.16501e+02	1.38912e −01	−4.11667e −05	1568.00	1622.00	2
AMBER	L15	B-2	2.80945e −01	9.48045e −05	−2.96085e −08	1619.00	2441.00	1
AMBER	L15	B-2	−1.86656e+02	2.29110e −01	−7.01678e −05	1568.00	1622.00	1
AMBER	L15	B-3	6.86425e −01	6.20320e −05	−3.42390e −08	1619.00	2444.00	2
AMBER	L15	B-3	−4.64569e+02	5.71654e −01	−1.75590e −04	1568.00	1622.00	2
AMBER	L15	C-2	4.41812e −01	4.65140e −05	−2.07239e −08	1619.00	2444.00	2
AMBER	L15	C-2	−2.42038e+02	2.96294e −01	−9.04966e −05	1568.00	1622.00	2
AMBER	L65	B-1	3.42255e −01	6.08407e −05	−5.67747e −09	3752.00	7077.00	1
AMBER	L65	B-1	−8.79137e+01	4.65463e −02	−6.12597e −06	3538.00	3755.00	1
AMBER	L65	B-2	2.08488e −01	5.94196e −05	−5.96003e −09	3752.00	7077.00	1
AMBER	L65	B-2	−8.24104e+01	4.42530e −02	−5.91574e −06	3538.00	3755.00	1
AMBER	L65	B-3	4.79409e −01	7.78557e −05	−7.63811e −09	3752.00	7077.00	1
AMBER	L65	B-3	−1.15509e+02	6.10988e −02	−8.03209e −06	3538.00	3755.00	1

Table 6: Summary of average FOS Aperture Coefficients [a]

Detec	FGWA	APER	C0	C1	C2	WMIN	WMAX	NAV
AMBER	L65	C-2	3.20407e −01	5.68714e −05	−5.89795e −09	3752.00	7077.00	1
AMBER	L65	C-2	−8.30983e+01	4.43141e −02	−5.87591e −06	3538.00	3755.00	1
AMBER	PRI	B-1	3.77070e −01	6.321 13e−06	−3.38474e −10	1618.00	7480.00	1
AMBER	PRI	B-1	−1.52755e+00	6.96870e −04	−5.86245e −08	7478.00	8890.00	1
AMBER	PRI	B-2	2.31237e −01	4.06172e −05	−4.24250e −09	1618.00	7480.00	1
AMBER	PRI	B-2	−7.26827e+00	2.04362e −03	−1.37986e −07	7478.00	8890.00	1
AMBER	PRI	B-3	5.61766e −01	−2.11169e−05	4.22438e −09	1618.00	7480.00	1
AMBER	PRI	B-3	−1.13509e+01	3.24538e −03	−2.19561e −07	7478.00	8890.00	1
AMBER	PRI	C-2	3.96385e −01	−7.60294e −06	1.73057e −09	1618.00	7480.00	1
AMBER	PRI	C-2	−6.45283e+00	1.92644e −03	−1.34419e −07	7478.00	8890.00	1

a. $A(ap) = C0 + C1 \times W + C2 \times W^2$, where W is the wavelength in Angstroms.

In order for a GO to understand the errors in the pipeline fluxes that are based on the NBH aperture corrections, the following list describes the major changes in order of decreasing numerical effect.

a) Over the small wavelength ranges for the four cases of detector -disperser modes with the secondary fits, the rapid drop in the aperture correction increases the calibrated fluxes by a factor of up to ~5.

b) NBH did not have measurements for the prisms and used the average for the high dispersion gratings. For example, the value for the B3(1.0 arcsec) aperture should be 0.53 instead of the 0.59 used by NBH for the blue side prism.

c) The biggest difference for the B3(1.0 arcsec) aperture between NBH and the T able 4 averages is for the high dispersion blue side average of 0.58 and the NBH value of 0.61 for blue H19.

d) A few of the smaller aperture transmission estimates are now ~10 percent larger than the NBH estimates; and the red side B2 aperture correction for L15 is 0.35 in T able 4, while the spuriously low NBH value of 0.29 was caused by large jitter that carried the star out of the 0.3 arcsec aperture for a significant fraction of the integration time.

V. Diffuse Sources

The above discussion of the relative aperture corrections of small apertures with respect to the 4.3 arcsec aperture for point sources is NOT relevant to absolute surface brightness estimates for diffuse sources. In terms of the inverse sensitivity ,

$S(4.3)$, of a point source at zero focus in the FOS 4.3 arcsec aperture, the flux of a point source with response, C, in counts/sec is

$$F = C \times S(4.3) / A(ap),$$

where A(ap) is the aperture correction defined by Table 6 for the aperture used to make the observation, where C is corrected to zero focus, and where A(4.3)=1 by definition. The inverse sensitivity S(ap)=S(4.3)/A(ap) is the calibration that actually resides in PODPS and that is distributed on request. The specific surface intensity, I, of a diffuse source that overfills an aperture with effective solid angle of omega(ap) is

$$I = C \times S(4.3) \times T(4.3) / omega(ap),$$

where the best estimates of the effective solid angle subtended by an aperture is still in Lindler, Bohlin, & Hartig (1985), where C is independent of focus and NOT corrected, and where $T(4.3)$ is the absolute transmission at zero focus of the 4.3 arcsec acquisition aperture that is used for the primary calibration observations of the standard stars. $T(4.3)$ cannot be measured directly but is estimated to be ~0.73 by Lindler & Bohlin (1993) and 0.70-0.72 by Evans (1993).

VI. Future Calibration Changes

Since there is little time left before the *HST* servicing mission, the new aperture corrections will not be immediately implemented in the PODPS pipeline reduction system. Instead, these new aperture corrections will be implemented along with the full scheme to handle the FOS changes in sensitivity with time that is in preparation by Lindler & Bohlin. Following the deployment of COSTAR, any reprocessing of old pre-COSTAR archival data will have the best estimates for FOS calibration parameters.

In the future, even after installation of the COSTAR optics, every absolute calibration observation should include aperture correction measurements for a couple of gratings in order to better characterize the repeatability of the relative throughput for any aperture that is normally used to make precise flux measurements of point sources. The blue side gratings H13 and H27 that have the biggest slopes in the prop 3106 data would be good choices for repeats in the B3 aperture. Since the aperture corrections are a function of grating and detector, all combinations must be done at least once following COSTAR deployment. Hopefully, these new aperture corrections will be more consistent with our expectations.

Ed Smith read a draft of this paper and provided several comments that improved the clarity and content.

References

Bohlin, R. C. 1993, FOS Instrument Science Report CAL/FOS-097.
Burrows, C., & Hasan, H. 1993, Telescope Image Modelling User Manual, Version 7c, Release 25 and updates through Release 28.
Evans, I. N. 1993, FOS Instrument Science Report CAL/FOS-105.
Fitch, J. E., Hartig, G. F., Beaver, E. A., and Hier, R. G. 1993, FOS Instrument Science Report CAL/FOS-098.
Koratkar, A., and Taylor, C. J. 1993, FOS Instrument Science Report CAL/FOS-096.
Lindler, D. J., & Bohlin, R. C. 1993, FOS Instrument Science Report CAL/FOS-102.
Lindler, D., Bohlin, R., & Hartig, G. 1985, FOS Instrument Science Report CAL/FOS-019.
Neill, J. D., Bohlin, R. C., & Hartig, G. 1992, FOS Instrument Science Report CAL/FOS-077 (NBH).